Synthesis and characterization of porphyrin sensitizers with various electron-donating substituents for highly efficient dye-sensitized solar cells†

Chou-Pou Hsieh,[a] Hsueh-Pei Lu,[b] Chien-Lan Chiu,[a] Cheng-Wei Lee,[a] Shu-Han Chuang,[a] Chi-Lun Mai,[a] Wei-Nan Yen,[a] Shun-Ju Hsu,[b] Eric Wei-Guang Diau*[b] and Chen-Yu Yeh*[a]

Received 21st September 2009, Accepted 5th November 2009
First published as an Advance Article on the web 16th December 2009
DOI: 10.1039/b919645e

A series of porphyrin dyes with an electron-donating group (EDG) attached at a *meso*-position (**YD1–YD8**) have been designed and synthesized for use as sensitizers in dye-sensitized solar cells (DSSC). The nature of the EDG exerts a significant influence on the spectral, electrochemical and photovoltaic properties of these sensitizers. Absorption spectra of porphyrins having an amino group show broadened Soret band and red-shifted Q bands with respect to those of reference porphyrin **YD0**. This phenomenon is more pronounced for porphyrins **YD7** and **YD8** that have a π-conjugated triphenylamine at the *meso*-position opposite the anchoring group. Upon introduction of an EDG at the *meso*-position, the potential for the first oxidation alters significantly to the negative whereas that for the first reduction changes inappreciably, indicating a decreased HOMO-LUMO gap. Results of density-functional theory (DFT) calculations support the spectroelectrochemical data for a delocalization of charge between the porphyrin ring and the amino group in the first oxidative state of diarylamino-substituted porphyrins **YD1–YD4**, which exhibit superior photovoltaic performance among all porphyrins under investigation. With long-chain alkyl groups on the diarylamino substituent, **YD2** shows the best cell performance with $J_{SC} = 13.4$ mA cm^{-2}, $V_{OC} = 0.71$ V, and $FF = 0.69$, giving an overall efficiency 6.6% of power conversion under simulated one-sun AM1.5 illumination.

Introduction

Dye-sensitized solar cells (DSSC) have attracted considerable attention over the past decade because they provide an economic alternative to silicon-based photovoltaic devices. The DSSC of ruthenium polypyridyl complexes produced an efficiency of solar-to-electric conversion up to 11% under standard global AM 1.5 solar conditions with enduring stability.[1] Several authors have modified the Ru-bipyridyl complexes to increase their conversion efficiencies since the discovery of the landmark N3 dye,[2] but, in view of the cost and environmental concern about ruthenium dyes, much effort has been directed to the development of organic dyes because of their modest cost, large absorption coefficient and the facile modification of their molecular structures.[3]

Numerous organic dyes have been synthesized for use in DSSC. Organic dyes with large conversion efficiencies are typically composed of a donor-π-conjugated unit-acceptor (D–π–A) structure with a well defined architecture.[4] These sensitizers include coumarin,[5] indoline,[6] oligoene,[7] thiophene,[8] triarylamine,[9] perylene,[10] cyanine[11] and hemicyanine[12] derivatives. Inspired by the efficient energy and electron transfer in the light-harvesting antenna of biological systems,[13] porphyrin derivatives[14] and analogues[15] have been widely used in photovoltaic devices. The intrinsic advantages of porphyrin-based dyes are their rigid molecular structures with large absorption coefficients in the visible region and their many reaction sites, *i.e.*, four *meso* and eight β positions, available for functionalization. Fine tuning of their optical, physical, and electrochemical properties thus becomes feasible.

On the basis of our previous work on the systematic modification of porphyrin dyes,[16] we found that the use of a phenylethynyl (PE) bridging unit between the porphyrin core and the carboxyl anchoring group *via* the *meso*-position results in broadening and red shift of absorption bands, and thus gives cell performance better than that of other bridges. In addition, porphyrin dyes substituted with a strong electron-donating diarylamino unit at the *meso*-position opposite the anchoring group exhibit a satisfactory cell performance comparable with that of the device made of N3 dye. To obtain insight into how the chemical and physical nature of the electron-donating groups influences the efficiency of power conversion, we systematically designed and prepared a series of porphyrin dyes with a D–π–A framework. Herein, we report the synthesis, spectral, electrochemical, and photovoltaic properties of six amine-substituted porphyrin sensitizers **YD2–YD6** and **YD8**, and the reference dyes **YD0**, **YD1**, and **YD7** (Figure 1).[16]

Results and discussion

Previous work showed that introduction of hydrophobic alkyl chains onto organic dyes suppresses the electron transfer from

[a]*Department of Chemistry, National Chung Hsing University, Taichung, 402, Taiwan. E-mail: cyyeh@dragon.nchu.edu.tw; Fax: +886 4-2286-2547; Tel: +886 4-2285-2264*
[b]*Department of Applied Chemistry, National Chiao Tung University, Hsinchu, 300, Taiwan. E-mail: diau@mail.nctu.edu.tw; Fax: +886 3-572-3764; Tel: +886 3-513-1524*

† Electronic Supplementary Information (ESI) available: Experimental details. See DOI: 10.1039/b919645e/

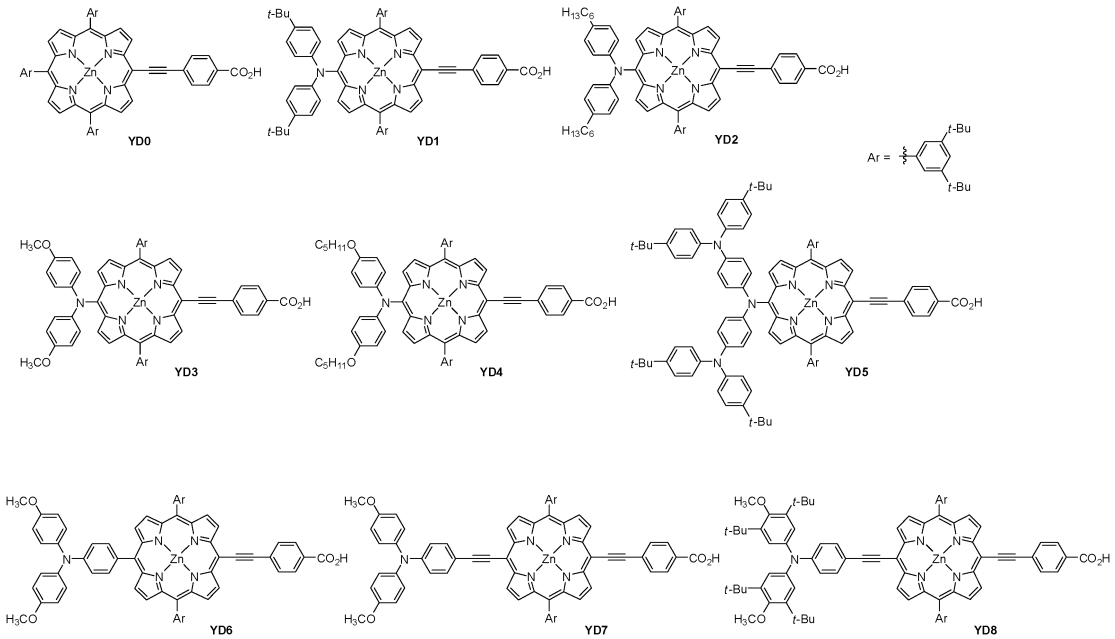

Fig. 1 Molecular structures of porphyrin dyes **YD0–YD8**.

TiO_2 to the electrolyte.[17] Compound **YD2** having two hexyl chains on the diphenylamine is expected to act as a more efficient sensitizer in a DSSC than **YD1**. Alkoxyl groups are considered to be stronger electron-donating groups than alkyl groups; accordingly, porphyrins **YD3** and **YD4** with methoxyl and pentoxyl groups, respectively, have been synthesized. Another promising strategy to increase the electron-donating ability of the porphyrin dye is to introduce a N-substituent onto the diarylamine moiety; compound **YD5** incorporated with a triamine group to the *meso*-position has also been synthesized. To extend the charge separation between porphyrin and TiO_2, porphyrins with a triarylamino group, **YD6–YD8**, have been designed and prepared. Our previous work showed that the cell performance of **YD7** is worse than that of **YD1**.[16] To see if this decreased efficiency might be ascribed to dye aggregation, we prepared **YD8** with four *tert*-butyl groups on triphenylamine. The syntheses of these porphyrin dyes are described in the supporting information.

The absorption spectra of these compounds are summarized in Table 1, and some representative examples are given in Figure 2. All porphyrin dyes in this work exhibit maxima attributed to π–π^* transitions in the range 400–500 nm for the Soret band and 550–750 nm for the Q bands. The molar absorption coefficients/10^5 M^{-1} cm^{-1} for the Soret band of these porphyrin dyes range from 1.36 to 4.98, so fulfilling one requirement for a dye usable in a DSSC, whereas those/10^3 M^{-1} cm^{-1} of the Q(0,0) band are in the range 16.9–52.7. The Soret and Q bands for **YD1–YD8** are broadened and red-shifted relative to those of **YD0**. Both Soret and Q(0,0) bands of **YD1–YD8** have full widths at half maximum (fwhm) height two or three times as large as those for the reference compound **YD0**; this effect is ascribed to an electronic interaction between the porphyrin core and the amino group. Both the Soret and Q bands for **YD1** and **YD2** show oscillator strengths comparable with that of **YD0**, although their absorption coefficients are much smaller than those of **YD0**. **YD5** exhibits a larger oscillator strength for both Soret and Q bands than for **YD0**. Among these porphyrins, **YD7** and **YD8** exhibit the most pronounced broadening and bathochromic shift of the Soret band, indicating that the acetylenic link effectively mediates the electronic coupling between the porphyrin and triarylamine units. Similar to the absorption, the emission is red-shifted on incorporation of an amino group onto the porphyrin macrocyle (Table 1).

We employed cyclic voltammetry to determine the redox potentials of these porphyrins; the electrochemical reactions of these compounds were measured under ambient conditions. The electrochemical data are summarized in Table 2. All porphyrin dyes exhibit reversible waves for the first oxidation, corresponding to the HOMO energy of the dye, at a potential greater than that of the I^-/I_3^- couple, which assures regeneration of the oxidized state.[18] Figure 3 shows representative cyclic voltammograms for **YD0**, **YD2**, **YD4**, **YD5**, **YD6**, and **YD8** in THF containing tetrabutylammonium hexafluorophosphate ($TBAPF_6$, 0.1 M). One reversible oxidation reaction was observed at $E_{1/2}$ = +1.04 V corresponding to the formation of $[\mathbf{YD0}]^+$ whereas an irreversible reduction wave was observed at about E_{pc} = −1.36 V. The potentials for the first and second oxidations of **YD1–YD5** show significant cathodic shifts with increasing electron-donating ability of the amino substituent as compared to those of **YD0**. For example, the first oxidation occurs at +1.04 V for **YD0**, shifts to +0.89 V for **YD2**, and further shifts to +0.77 V for **YD4**, whereas the reduction potential occurs at E_{pc} = −1.36 V for **YD0** and in a small range −1.00 to −1.20 V for **YD1–YD8**. Incorporation of an amino group onto the porphyrin ring decreases the electrochemical HOMO energy gap, consistent with red shifts of both Soret and Q bands in the absorption spectra. In our previous work, both porphyrin and diarylamino units were responsible for the first and second oxidations of **YD1** because the electron density of HOMO and HOMO-1 is distributed to these two units.[16] Similarly, the

Table 1 Absorption, fluorescence and electrochemical data for porphyrins **YD0–YD8**.[a]

Porphyrins	fwhm,[b] B-band/cm^{-1}	f_B[c]	fwhm, Q-band/cm^{-1}	f_Q[d]	Absorption λ_{max}[nm](ε[10^{3}M^{-1}cm^{-1}])	Emission λ_{max}[nm]
YD0	672	1.46	540	0.15	442(498), 579(16.8), 627(39.8)	634[e]
YD1	1708	1.36	914	0.15	442(207), 587(11.1), 644(31.2)	672[e]
YD2	1700	1.42	934	0.15	444(217), 589(10.8), 648(33.7)	676[f]
YD3	1366	0.88	1170	0.10	440(141), 592(5.9), 664(16.9)	701[f]
YD4	1313	0.86	1169	0.10	438(143), 591(5.4), 665(17.6)	701[f]
YD5	1088	1.55	1592	0.20	441(307), 659(27.2)	687[g]
YD6	1217	0.76	634	0.07	443(216), 579(8.0), 628(20.8)	641[f]
YD7	2042	1.05	898	0.20	449(141), 672(52.7)	689[g]
YD8	1940	0.95	876	0.17	457(136), 671(49.9)	689[g]

[a] Absorption and emission data were measured in ethanol for **YD0–YD6**, and in THF for **YD7** and **YD8** at 25 °C. [b] fwhm denotes the full width at half-maximum height. [c] Oscillator strengths calculated over the region from 400 to 550 nm. [d] Oscillator strengths calculated over the region from 550 to 750 nm. [e] The excitation wavelengths were 550 nm. [f] The excitation wavelengths were 600 nm. [g] The excitation wavelengths were 650 nm.

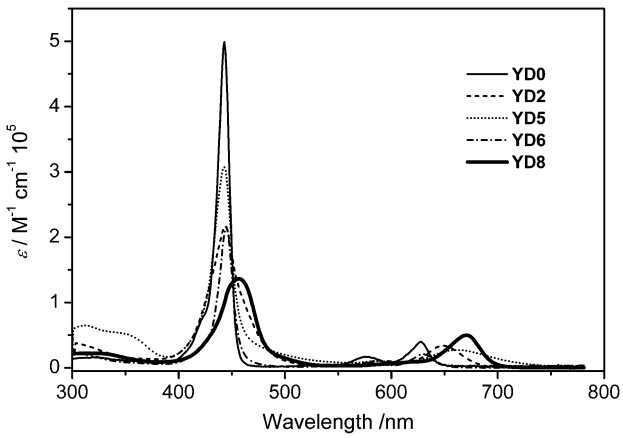

Fig. 2 UV-visible absorption spectra of **YD0**, **YD2**, **YD5** and **YD6** in ethanol, and **YD8** in THF.

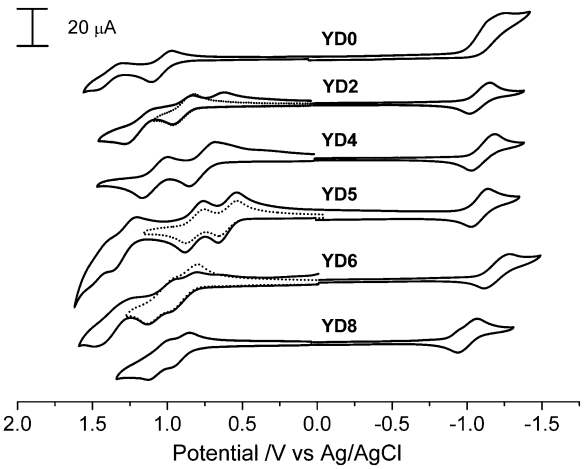

Fig. 3 Cyclic voltammograms of **YD0**, **YD2**, **YD4**, **YD5**, **YD6**, and **YD8** in THF containing 0.1 M $TBAPF_6$ at 25 °C.

Table 2 Electrochemical data for porphyrins **YD0–YD8**.[a]

Porphyrins	Oxidation $E_{1/2}$/V	Reduction $E_{1/2}$/V
YD0	+1.04, +1.48[b]	−1.36[b]
YD1	+0.92, +1.29[b]	−1.07
YD2	+0.89, +1.29[b]	−1.09
YD3	+0.81, +1.22[b]	−1.20[b]
YD4	+0.77, +1.08	−1.10
YD5	+0.60, +0.80, +1.29, +1.46	−1.08
YD6	+0.88, +1.05, +1.49[b]	−1.19
YD7	+0.91, +1.06	−1.01
YD8	+0.89, +1.05	−1.03

[a] Electrochemical measurements were performed at 25 °C in THF containing $TBAPF_6$ (0.1 M) as supporting electrolyte. Potentials measured *vs.* ferrocene/ferrocenium (Fc/Fc^+) couple were converted to normal hydrogen electrode (NHE) by addition of +0.63 V. [b] Irreversible process E_{pa} or E_{pc}.

first and second oxidations for **YD2–YD4** involve charge delocalization through the porphyrin ring and diarylamino moiety, which is further confirmed by DFT calculations.

The cyclic voltammogram of **YD5** shows four oxidation waves at $E_{1/2}$ = +0.60, +0.80, +1.29 and +1.46 V, respectively. The oxidations of the triamine component occur at +0.60, +0.80 and +1.28 V. The first and second oxidation centers for **YD5** are thus assignable to the triamine unit, consistent with DFT calculations that show the HOMO and HOMO-1 to be located on the donor subunit. The third and fourth oxidations at +1.29 and +1.46 V might involve both porphyrin and triamine units. Compound **YD6** shows two reversible couples at +0.88 and +1.05 V corresponding to oxidations from the triarylamine unit and the porphyrin ring, respectively. The irreversible wave at +1.49 V is assigned to the second electron abstraction from the porphyrin core. Compounds **YD7** and **YD8** exhibit a similar electrochemical behaviour with two reversible oxidations occurring about +0.90 and +1.05 V. Our previous electrochemical measurements on **YD7** showed that the first oxidation occurs at the triarylamine unit and the second electron abstraction corresponds to the oxidation of the porphyrin ring.[16]

The excited-state oxidation potentials (E_{0-0}*) are obtained from the relation $E_{0-0}^* = E_{ox1} - E_{0-0}$, in which E_{ox1} is the first oxidation potential of a porphyrin dye and E_{0-0} is the zero-zero excitation energy obtained from the absorption edge.[18,19] The energy levels of these porphyrins are depicted in Figure 4. The calculated E_{0-0}* values are all more negative than the conduction edge (–0.50 V *vs.* NHE) of TiO_2, which is compatible with electron injection from the excited state of the dye to the conduction

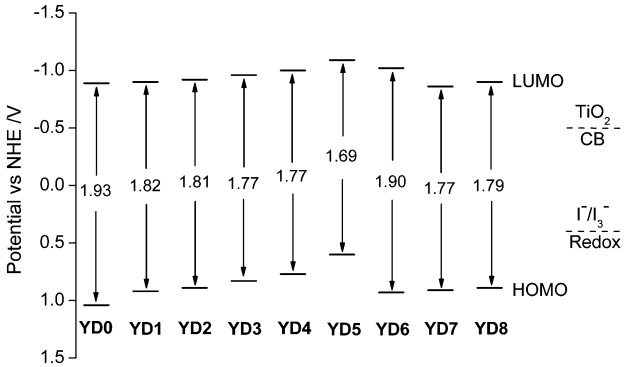

Fig. 4 A schematic energy-level diagram of porphyrins **YD0–YD8**. HOMO = E_{ox1} and LUMO = $E_{0\text{–}0}$*.

band (CB) of TiO_2. As the HOMO levels are more positive than the oxidation potential for I^-/I_3^- (+0.40 V *vs.* NHE), the energy levels for **YD1–YD8** all fulfil the requirement for effective electron injection and dye regeneration in a DSSC system.

To gain insight into the electron distribution of the frontier and other close-lying orbitals, we performed quantum-chemical calculations on some porphyrins using density-functional theory (DFT) at the B3LYP/6-31G(d) level (Spartan 08 package). To simplify the computations, the alkyl groups of phenyl rings were replaced by hydrogen atoms or methyl groups. Figure 5 shows an energy-level diagram and the corresponding molecular orbitals for these porphyrin dyes. There is a discrepancy between the HOMO-LUMO gaps shown in Figures 4 and 5 because the electron correlation and the solvent effect have not been taken into account. Figure 4 shows a reduced HOMO-LUMO gap upon incorporation of an electron-donating group to the porphyrin ring, which is in accordance with the tendency on the change of the HOMO-LUMO gap calculated from DFT.

In the electronic absorption for a porphyrin, both Soret and Q bands arise from π–π* transitions, which can be explained by considering the Gouterman four-orbital model: two π orbitals (a_{1u} and a_{2u}) and two degenerate π* orbitals (e_{gx} and e_{gy}).[20] In compounds **YD1–YD8**, there is considerable electronic coupling between the electron-donating group and the porphyrin core, thus decreasing the HOMO-LUMO energy gaps relative to **YD0**. This effect is consistent with the red shift in absorption and emission upon introduction of an electron-donating group onto the porphyrin ring. The separation between the a_{1u} and a_{2u} orbitals increased upon introduction of a donor group whereas the energy splitting of the e_{gx}/e_{gy} pair was only slightly perturbed.

According to our previous work,[16] the electronic density of **YD1** is significantly distributed into the π-system of the porphyrin ring and the diphenylamino moiety at the HOMO and HOMO-1. Introduction of a more strongly electron-donating group would increase the electronic density on the diarylamino moiety. The HOMO of **YD3** shows an increased electron distribution located on the electron-donating diarylamine relative to **YD2**. Similar to the LUMO of **YD2**, the π-conjugation is extended to only the porphyrin ring and the phenylene link at the LUMO of **YD3**. Comparison of **YD1**, **YD3** and **YD5** with **YD0** shows that increasing the electron-donating ability of the amino substituents results in a decreased HOMO-LUMO gap, which is ascribed to the significantly elevated HOMO as the LUMO is moderately altered. The HOMO electronic densities of **YD5** and **YD6** are significantly distributed on the triamine and triarylamine moieties, respectively; the LUMO shows an electronic distribution on both the porphyrin and phenylene units. In the case of **YD7**, for which the triarylamine is attached at the *meso*-position through an acetylene link, the distribution of electronic density of the molecular orbitals is similar to that of **YD6**.

The primary step of charge separation in DSSC is electron injection from the excited state of the dye into the conduction band of TiO_2, which generates the dye cation. To improve our understanding of the electronic absorption properties of the oxidized species, we investigated the electrochemical reactions of these porphyrin dyes with a spectroelectrochemical method. The spectroelectrochemical properties of **YD1** and **YD7** have been previously investigated.[16] Upon oxidation, the positive charge of **YD1** is delocalized over both the porphyrin and diarylamino units whereas that of **YD7** is localized on the triarylamino moiety. According to the DFT calculations, the spectroelectrochemical behaviours of **YD2–YD4** are expected to resemble that of **YD1**. Figure 6 shows scans of absorption spectra of **YD2** as a thin layer obtained during electrochemical oxidation at an applied potential from +0.40 to +0.98 V in THF containing $TBAPF_6$ (0.1 M) at 25 °C. As expected, the Soret band at 443 nm decreases while a band at 813 nm and a broad band at 1329 nm increase in the course of electrolysis at applied potential of +0.98 V. The band at 813 nm is characteristic of a porphyrin cation. Such a band in this region has also been observed in a bis-(diphenylamino)-substituted porphyrin upon 1 e^- oxidation.[21] As shown in Figure 5, the electron density of HOMO for the **YD2** is mainly distributed on the diphenylamine and porphyrin units. The charge would delocalize over the porphyrin ring and the diphenylamine moiety upon 1 e^- oxidation. Therefore, the broad band at 1329 nm may correspond to the intervalence state.[22] The first oxidation is essentially reversible as more than 90% of the oxidized species generated at +0.98 V can be reconverted to the neutral form of **YD2** according to the intensity of the Q band whereas the second oxidation at +1.35 V is irreversible.

Figure 7 shows the spectral changes of porphyrin **YD5** at applied potentials +0.73 and +1.14 V in THF containing $TBAPF_6$ (0.1 M) at 25 °C. In the first oxidation, the Soret band at 444 nm and the signal at 304 nm corresponding to the triamine unit decrease while those at 860 and 1404 nm increase, with clear isosbestic points. The Q_x and Q_y bands become visible and shifted to 570 and 628 nm upon oxidation of **YD5**. As compared to **YD2**, which shows a sharp decrease in the Soret band, **YD5** exhibits a moderate decrease in the Soret band upon oxidation because the first oxidation is assigned to a triamine-centred electrochemical reaction on the basis of quantum-chemical calculations (Figure 5). A previous report on the spectroelectrochemical properties of triamine systems showed that a moderate band at about 700 nm and a broad absorption at about 1250 nm appear corresponding to the intervalence state upon 1 e^- oxidation.[22] The 860 nm band for [**YD5**]$^+$ may be caused by the triamine cation unit. Further oxidation at +1.14 V results in a decreased wavelength of the Soret band and the appearance of a new broad band at ~1010 nm. As shown in Figure 5, the electron density of the HOMO and HOMO-1 orbitals is mainly distributed on the triamine unit. Thus, the second oxidation at +1.14 V for **YD5** is assigned to the second

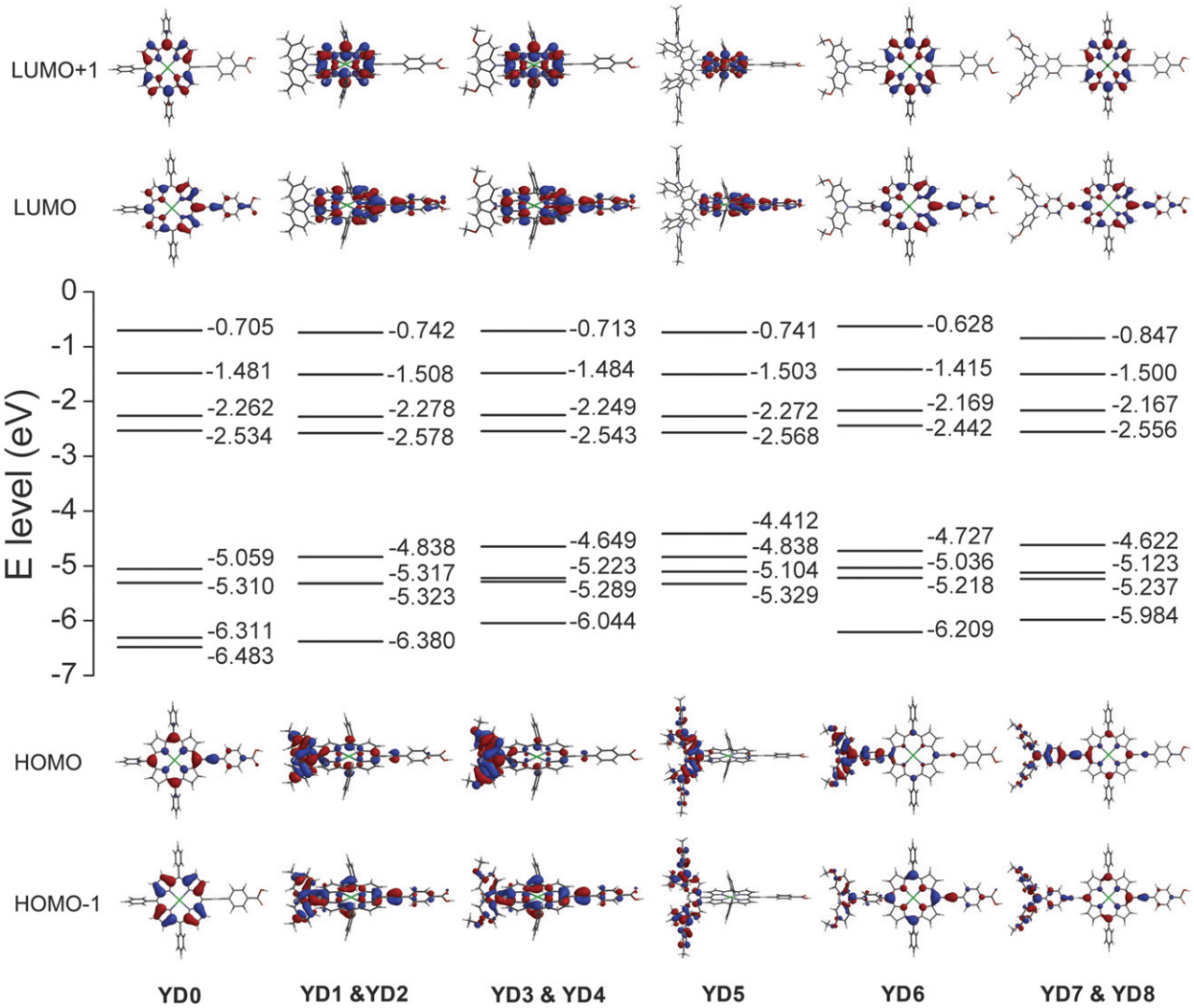

Fig. 5 Energy-level diagram and the corresponding molecular orbitals of porphyrins **YD0–YD8** calculated at the B3LYP/6-31G(d) level of theory.

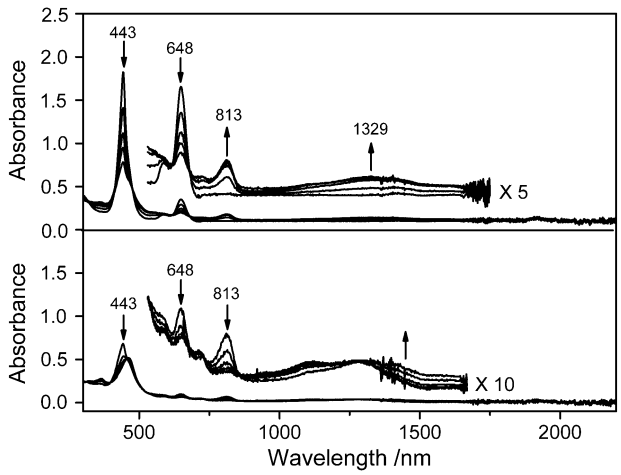

Fig. 6 Spectral changes of **YD2** in THF containing $TBAPF_6$ (0.1 M) at applied potentials +0.98 V (top), and +1.35 V (bottom); the electrolysis time for each process is about 30 min.

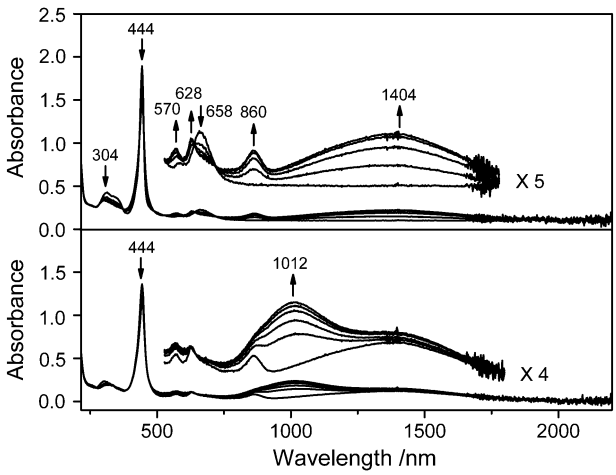

Fig. 7 Spectral changes of **YD5** in THF containing $TBAPF_6$ (0.1 M) at applied potentials +0.73 V (top), and +1.14 V (bottom); the electrolysis time for each process is about 30 min.

electron abstraction from the triamine moiety. The broad bands in the near IR region for the oxidized species (~1400 nm for $[\mathbf{YD5}]^+$, and ~1010 and ~1400 nm for $[\mathbf{YD5}]^{2+}$) might be attributed to both the intervalence states within the triamine unit and the charge transfer from the porphyrin ring to the triamine cation. These oxidation processes are reversible because more than 95% of the oxidized species is reconverted to the neutral form of **YD5**.

The spectroelectrochemical measurements of **YD6** were also performed in THF under ambient conditions (Figure 8). Unlike $[\mathbf{YD2}]^+$ and $[\mathbf{YD5}]^+$ for which a broad band in the near IR region was observed, $[\mathbf{YD6}]^+$ shows no absorption at a wavelength greater than 800 nm. Scans of UV-visible spectra exhibit a new band at ~740 nm for the first electron abstraction; furthermore, the intensities of the Soret and Q bands decrease for the first and second oxidations. The first and second oxidations likely correspond to 1 e^- abstraction from each of the triarylamine and porphyrin units, respectively, on the basis of DFT calculations.

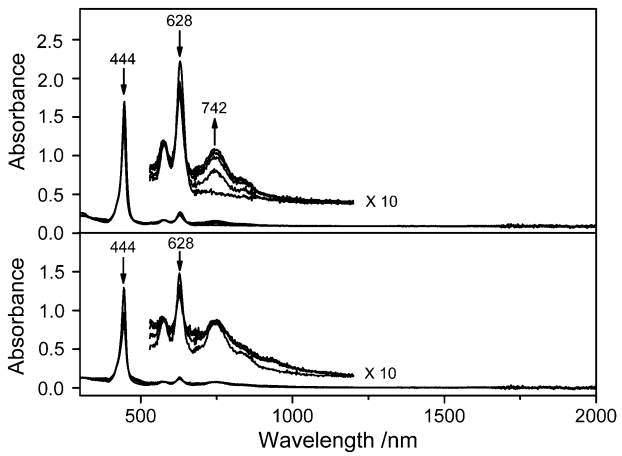

Fig. 8 Spectral changes of **YD6** in THF containing $TBAPF_6$ (0.1 M) at applied potentials +0.98 V (top), and +1.15 V (bottom); the electrolysis time for each process is about 30 min.

Porphyrins **YD0–YD8** were sensitized onto TiO_2 nanoparticulate films to serve as working electrodes of DSSC devices for photovoltaic characterization. Figure 9a shows the transmittance absorption spectra of the sensitized thin-film samples in three parts; Figures 9b and 9c show the corresponding action spectra and current-voltage curves of the devices, respectively. The thin-film samples show much broader absorption (Figure 9a) than their solution counterparts (Figure 1) because of strong intermolecular interactions of the molecules aggregated on TiO_2 surface. The large absorbances of the thin-film spectra indicate that the amounts of dye loading on TiO_2 films were sufficient for all porphyrin sensitizers. The IPCE action spectra (Figure 9b) reflect the photoelectric conversion efficiency at each wavelength. Although there is a large gap between the Soret and the Q bands of the absorption spectra of porphyrins, this feature is not evident in the IPCE spectra because the scattering by TiO_2 nanoparticles increases the photocurrents for the weak absorption in that region.

Table 3 summarizes the photovoltaic parameters derived from Figure 9c for devices **YD0–YD8**. The overall efficiencies of power conversion of the devices exhibit a systematic trend for porphyrins with varied *meso*-substituents according to three classes. First, the diarylamino groups substituted directly on the *meso*-position, *i.e.*, **YD1–YD4**, show a cell performance much better than for our reference cell, **YD0**. Second, the triarylamino-substituted porphyrins, **YD6–YD8**, exhibit cell performance comparable to that of **YD0**. Third, the triamine-substituted porphyrin, **YD5**, displays cell performance much poorer than that of **YD0**. We discuss the observed photovoltaic sequence of **YD1–YD8** in what follows.

Because the π-conjugation of the diarylamino groups extends the spectral absorption towards long wavelength, the photocurrents of **YD1–YD4** are significantly greater than that of **YD0**; the long-chain hydrocarbons further extend the spectral region of light harvesting and make the performance of **YD2** slightly larger than **YD1** and that of **YD4** slightly greater than **YD3**. Although both **YD3** and **YD4** have alkoxyl groups on the diarylamino substituent, the additional electron-donating groups increased no further the device performance. The action spectra shown in

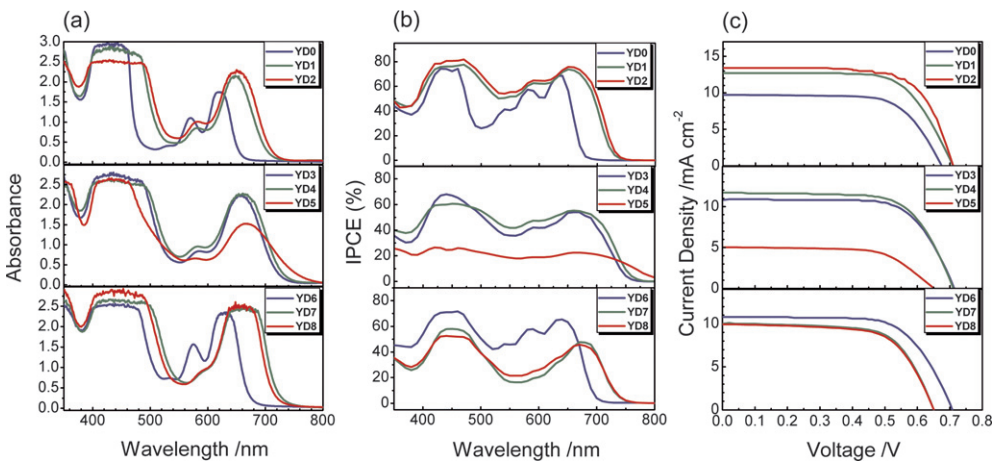

Fig. 9 (a) Absorption spectra of films with no added scattering layer (film thickness ~10 μm), (b) incident photon-to-current conversion efficiency (IPCE) spectra of devices, and (c) current-voltage characteristics of devices fabricated from **YD0–YD8** sensitized on TiO_2 films (film thickness ~(10 + 4) μm).

Table 3 Photovoltaic parameters of porphyrin-based dye-sensitized solar cells under AM1.5 illumination (power 100 mW cm^{-2}) and active area 0.16 cm^2

Porphyrins	J_{SC}/mA cm^{-2}	V_{OC}/V	*FF*	η (%)
YD0	9.45	0.675	0.68	4.34
YD1	12.73	0.710	0.68	6.15
YD2	13.40	0.710	0.69	6.56
YD3	10.85	0.713	0.69	5.34
YD4	11.68	0.711	0.68	5.65
YD5	5.05	0.651	0.64	2.10
YD6	10.81	0.708	0.67	5.13
YD7	10.05	0.650	0.67	4.38
YD8	9.94	0.651	0.66	4.27

Figure 9b indicate that the efficiency values of **YD3** and **YD4** are less than those of **YD1** and **YD2**, which accounts for the J_{SC} values of the former being smaller than those of the latter. This decrease might reflect that the additional electron-donating groups raise the energy level of the HOMO (Figures 4 and 5) so that dye regeneration of the porphyrin cations from the electrolyte becomes slower. Such an effect became more pronounced when a more strongly electron-donating group was present. For example, **YD5** has a triamine substituent, which is a stronger electron-donating group than a diarylamine, so that the HOMO level is the highest among all porphyrins under investigation. As a result, **YD5** shows a small J_{SC} value that is confirmed by its significantly smaller efficiency through the entire action spectrum shown in the middle panel of Figure 9b.

YD7 and **YD8** also have excellent π-conjugation between the porphyrin core and the phenyl group through the CC triple-bond bridge so that their thin-film absorption spectra are similar to those of **YD1–YD4** (Figure 9a), but their device performances are poorer than those of **YD1–YD4**. **YD7** suffered from dye aggregation in ethanol solution;[16] additional *tert*-butyl groups in **YD8** failed to decrease the tendency of aggregation. The smaller J_{SC} and V_{OC} of **YD7** and **YD8** are thus expected to be due to the effect of dye aggregation so that fewer electrons were injected into the conduction band of TiO_2 after photoexcitation. In contrast, the structure of **YD6** has a triarylamino group directly attached at the *meso*-position of the porphyrin core without a triple bond as a bridge; rotation about the bridged C–C single bond is thus feasible so that effective π-conjugation between the porphyrin core and the triarylamine substituent was unattainable (Figure 5). As a result, the thin-film absorption spectrum of **YD6** is similar to that of **YD0**, but the electron-donating ability of the triarylamino group increases the efficiency of the former relative to the latter to improve the cell performance of the former.

The electron-donating feature of amino substituents in **YD1–YD4** and **YD6** seems to be responsible for the V_{OC} value (~0.71 V) being larger than that (0.675 V) of the reference cell (**YD0**). Among evidence from other work, Durrant and co-workers found that the period for charge recombination of a triarylamino porphyrin/TiO_2 film is 20 times that of a free-base porphyrin counterpart (80 *vs.* 4 ms);[23] Mozer *et al.* noted that the smaller V_{OC} of porphyrin-sensitized solar cells is due to the decreased electron lifetime related to either a more rapid recombination of electrons with dye cations or I_3^- ions.[24] We therefore expect that the observed larger V_{OC} in **YD1–YD4** and **YD6** compared to **YD0** is due to a diminished recombination between I_3^- and conduction-band electrons, because I_3^- might be attached to the positively charged diarylamino moiety far from the TiO_2 surface for the former case. For **YD7** and **YD8**, although the amino group is farther from TiO_2 than in the cases of **YD1–YD4** and the electron distribution of the frontier orbitals is appropriate for their use in DSSC (Figure 5), the V_{OC} values of **YD7** and **YD8** (~0.65 V) are smaller than those of **YD1–YD4**, and even smaller than those of **YD0** because of the effect of aggregation.

Conclusions

We have synthesized new porphyrin dyes with a donor group attached at the *meso*-position of the porphyrin for dye-sensitized solar cells. The tuning of the HOMO-LUMO energy gap, thus the optical and electrochemical properties, is achievable on varying the structure of the donor group. The electronic interaction between the donor and the porphyrin units in **YD1–YD8** significantly affects the spectral features of absorption and electrochemical properties. Our results reveal that direct attachment of an alkyl-substituted diarylamino group to the porphyrin ring results in significant improvement in solar-to-electrical conversion efficiency. This work provides a basis for the future design and synthesis of more efficient porphyrin-based DSSC.

Acknowledgements

National Science Council of Taiwan and Ministry of Education of Taiwan, under the ATU program, provided support for this project.

References

1 (*a*) B. O'Regan and M. Grätzel, *Nature*, 1991, **353**, 737; (*b*) M. K. Nazeeruddin, A. Kay, I. Rodicio, R. Humphry-Baker, E. Müller, P. Liska, N. Vlachopoulos and M. Grätzel, *J. Am. Chem. Soc.*, 1993, **115**, 6382; (*c*) M. K. Nazeeruddin, P. Péchy, T. Renouard, S. M. Zakeeruddin, R. Humphry-Baker, P. Comte, P. Liska, L. Cevey, E. Costa, V. Shklover, L. Spiccia, G. B. Deacon, C. A. Bignozzi and M. Grätzel, *J. Am. Chem. Soc.*, 2001, **123**, 1613.

2 (*a*) C.-Y. Chen, S.-J. Wu, J.-Y. Li, C.-G. Wu, J.-G. Chen and K.-C. Ho, *Adv. Mater.*, 2007, **19**, 3888; (*b*) C.-Y. Chen, J.-G. Chen, S.-J. Wu, J.-Y. Li, C.-G. Wu and K.-C. Ho, *Angew. Chem., Int. Ed.*, 2008, **47**, 7342; (*c*) F. Gao, Y. Wang, D. Shi, J. Zhang, M. Wang, X. Jing, R. Humphry-Baker, P. Wang, S. M. Zakeeruddin and M. Grätzel, *J. Am. Chem. Soc.*, 2008, **130**, 10720; (*d*) Y. Cao, Y. Bai, Q. Yu, Y. Cheng, S. Liu, D. Shi, F. Cao and P. Wang, *J. Phys. Chem. C*, 2009, **113**, 6290.

3 Y. Ooyama and Y. Harima, *Eur. J. Org. Chem.*, 2009, 2903.

4 (*a*) K. Hara, K. Sayama, Y. Ohga, A. Shinpo, S. Suga and H. Arakawa, *Chem. Commun.*, 2001, 569; (*b*) K. Hara, M. Kurashige, S. Ito, A. Shinpo, S. Suga, K. Sayama and H. Arakawa, *Chem. Commun.*, 2003, 252; (*c*) Z.-S. Wang, Y. Cui, K. Hara, Y. Dan-ho, C. Kasada and A. Shinpo, *Adv. Mater.*, 2007, **19**, 1138; (*d*) A. Mishra, M. K. R. Fischer and P. Bäuerle, *Angew. Chem., Int. Ed.*, 2009, **48**, 2474.

5 (*a*) K. Hara, M. Kurashige, Y. Danoh, C. Kasada, A. Shinpo, S. Suga, K. Sayama and H. Arakawa, *New J. Chem.*, 2003, **27**, 783; (*b*) Z.-S. Wang, Y. Cui, Y. Dan-oh, C. Kasada, A. Shinpo and K. Hara, *J. Phys. Chem. C*, 2007, **111**, 7224.

6 (*a*) T. Horiuchi, H. Miura and S. Uchida, *Chem. Commun.*, 2003, 3036; (*b*) T. Horiuchi, H. Miura, K. Sumioka and S. Uchida, *J. Am. Chem. Soc.*, 2004, **126**, 12218; (*c*) S. Ito, S. M. Zakeeruddin, R. Humphry-Baker, P. Liska, R. Charvet, P. Comte,

M. K. Nazeeruddin, P. Péchy, M. Takata, H. Miura, S. Uchida and M. Grätzel, *Adv. Mater.*, 2006, **18**, 1202.
7 (*a*) T. Kitamura, M. Ikeda, K. Shigaki, T. Inoue, N. A. Anderson, X. Ai, T. Lian and S. Yanagida, *Chem. Mater.*, 2004, **16**, 1806; (*b*) K. Hara, T. Sato, R. Katoh, A. Furabe, T. Yoshihara, M. Murai, M. Kurashige, S. Ito, A. Shinpo, S. Suga and H. Arakawa, *Adv. Funct. Mater.*, 2005, **15**, 246.
8 (*a*) S. Kim, H. Choi, D. Kim, K. Song, S. O. Kang and J. Ko, *Tetrahedron*, 2007, **63**, 9206; (*b*) S. Kim, H. Choi, C. Baik, K. Song, S. O. Kang and J. Ko, *Tetrahedron*, 2007, **63**, 11436; (*c*) I. Jung, J. K. Lee, K. H. Song, K. Song, S. O. Kang and J. Ko, *J. Org. Chem.*, 2007, **72**, 3652.
9 (*a*) M. Velusamy, K. R. J. Thomas, J. T. Lin, Y. Hsu and K. Ho, *Org. Lett.*, 2005, **7**, 1899; (*b*) D. P. Hagberg, T. Edvinsson, T. Marinado, G. Boschloo, A. Hagfeldt and L. Sun, *Chem. Commun.*, 2006, 2245; (*c*) M. Liang, W. Xu, F. Cai, P. Chen, B. Peng, J. Chen and Z. Li, *J. Phys. Chem. C*, 2007, **111**, 4465.
10 (*a*) S. Ferrere, A. Zaban and B. A. Greg, *J. Phys. Chem. B*, 1997, **101**, 4490; (*b*) S. Ferrere and B. A. Greg, *New J. Chem.*, 2002, **26**, 1155; (*c*) Y. Shibano, T. Umeyama, Y. Matano and H. Imahori, *Org. Lett.*, 2007, **9**, 1971.
11 (*a*) A. Ehret, L. Stuhl and M. T. Spitler, *J. Phys. Chem. B*, 2001, **105**, 9960; (*b*) S. Ushiroda, N. Ruzycki, Y. Lu, M. T. Spitler and B. A. Parkinson, *J. Am. Chem. Soc.*, 2005, **127**, 5158; (*c*) S. Tatay, S. A. Haque, B. O'Regan, J. R. Durrant, W. J. H. Verhees, J. M. Kroon, A. Vidal-Ferran, P. Gaviña and E. Palomares, *J. Mater. Chem.*, 2007, **17**, 3037.
12 (*a*) Q.-H. Yao, L. Shan, F.-Y. Li, D.-D. Yin and C.-H. Huang, *New J. Chem.*, 2003, **27**, 1277; (*b*) Y.-S. Chen, C. Li, Z.-H. Zeng, W.-B. Wang, X.-S. Wang and B.-W. Zhang, *J. Mater. Chem.*, 2005, **15**, 1654.
13 J. Deisenhofer and J. R. Norris, *The Photosynthetic Reaction*, Academic Press, New York, 1993.
14 (*a*) T. Hasobe, H. Imahori, P. V. Kamat, T. K. Ahn, S. K. Kim, D. Kim, A. Fujimoto, T. Hirakawa and S. Fukuzumi, *J. Am. Chem. Soc.*, 2005, **127**, 1216; (*b*) T. Hasobe, P. V. Kamat, V. Troiani, N. Solladié, T. K. Ahn, S. K. Kim, D. Kim, A. Kongkanand, S. Kuwabata and S. Fukuzumi, *J. Phys. Chem. B*, 2005, **109**, 19; (*c*) M. Borgström, E. Blart, G. Boschloo, E. Mukhtar, A. Hagfeldt, L. Hammarström and F. Odobel, *J. Phys. Chem. B*, 2005, **109**, 22928; (*d*) L. Luo, C.-F. Lo, C.-Y. Lin, I.-J. Chang and E. W.-G. Diau, *J. Phys. Chem. B*, 2006, **110**, 410; (*e*) A. Huijser, T. J. Savenije, A. Kotlewski, S. J. Picken and L. D. A. Siebbeles, *Adv. Mater.*, 2006, **18**, 2234; (*f*) O. Hagemann, M. Jørgensen and F. C. Krebs, *J. Org. Chem.*, 2006, **71**, 5546; (*g*) G. M. Hasselman, D. F. Watson, J. R. Stromberg, D. F. Bocian, D. Holten, J. S. Lindsey and G. J. Meyer, *J. Phys. Chem. B*, 2006, **110**, 25430; (*h*) J. Rochford, D. Chu, A. Hagfeldt and E. Galoppini, *J. Am. Chem. Soc.*, 2007, **129**, 4655; (*i*) S. Eu, S. Hayashi, T. Umeyama, A. Oguro, M. Kawasaki, N. Kadota, Y. Matano and H. Imahori, *J. Phys. Chem. C*, 2007, **111**, 3528; (*j*) W. M. Campbell, K. W. Jolley, P. Wagner, K. Wagner, P. J. Walsh, K. C. Gordon, L. Schmidt-Mende, M. K. Nazeeruddin, Q. Wang, M. Grätzel and D. L. Officer, *J. Phys. Chem. C*, 2007, **111**, 11760; (*k*) S. Eu, S. Hayashi, T. Umeyama, Y. Matano, Y. Araki and H. Imahori, *J. Phys. Chem. C*, 2008, **112**, 4396; (*l*) J. K. Park, H. R. Lee, J. Chen, H. Shinokubo, A. Osuka and D. Kim, *J. Phys. Chem. C*, 2008, **112**, 16691; (*m*) S. Hayashi, M. Tanaka, H. Hayashi, S. Eu, T. Umeyama, Y. Matano, Y. Araki and H. Imahori, *J. Phys. Chem. C*, 2008, **112**, 15576; (*n*) C.-Y. Lin, C.-F. Lo, L. Luo, H.-P. Lu, C.-S. Hung and E. W.-G. Diau, *J. Phys. Chem. C*, 2009, **113**, 755.
15 (*a*) B. C. O'Regan, I. López-Duarte, M. V. Martínez-Díaz, A. Forneli, J. Albero, A. Morandeira, E. Palomares, T. Torres and J. R. Durrant, *J. Am. Chem. Soc.*, 2008, **130**, 2906; (*b*) J.-J. Cid, J.-H. Yum, S.-R. Jang, M. K. Nazeeruddin, E. Martínez-Ferrero, E. Palomares, J. Ko, Michael Grätzel and T. Torres, *Angew. Chem., Int. Ed.*, 2007, **46**, 8358; (*c*) P. Y. Reddy, L. Giribabu, C. Lyness, H. J. Snaith, C. Vijaykumar, M. Chandrasekharam, M. Lakshmikantam, J.-H. Yum, K. Kalyanasundaram, M. Grätzel and M. K. Nazeeruddin, *Angew. Chem., Int. Ed.*, 2007, **46**, 373; (*d*) J. He, G. Benkö, F. Korodi, T. Polívka, R. Lomoth, B. Åkermark, L. Sun, A. Hagfeldt and V. Sundström, *J. Am. Chem. Soc.*, 2002, **124**, 4922; (*e*) E. Palomares, M. V. Martínez-Díaz, Saif A. Haque, T. Torres and J. R. Durrant, *Chem. Commun.*, 2004, 2112.
16 C.-W. Lee, H.-P. Lu, C.-M. Lan, Y.-L. Huang, Y.-R. Liang, W.-N. Yen, Y.-C. Liu, Y.-S. Lin, E. W.-G. Diau and C.-Y. Yeh, *Chem.–Eur. J.*, 2009, **15**, 1403.
17 (*a*) N. Koumura, Z.-S. Wang, S. Mori, M. Miyashita, E. Suzuki and K. Hara, *J. Am. Chem. Soc.*, 2006, **128**, 14256; (*b*) Z.-S. Wang, N. Koumura, Y. Cui, M. Takahashi, H. Sekiguchi, A. Mori, T. Kubo, A. Furube and K. Hara, *Chem. Mater.*, 2008, **20**, 3993.
18 D. P. Hagberg, J.-H. Yum, H. Lee, F. D. Angelis, T. Marinado, K. M. Karlsson, R. Humphry-Baker, L. Sun, A. Hagfeldt, M. Grätzel and M. K. Nazeeruddin, *J. Am. Chem. Soc.*, 2008, **130**, 6259.
19 J. K. Park, H. R. Lee, J. Chen, H. Shinokubo, A. Osuka and D. Kim, *J. Phys. Chem. C*, 2008, **112**, 16691.
20 H. L. Anderson, *Chem. Commun.*, 1999, 2323.
21 R. Sakamoto, T. Sasaki, N. Honda and T. Yamamura, *Chem. Commun.*, 2009, 5156.
22 Y. Hirao, A. Ito and K. Tanaka, *J. Phys. Chem. A*, 2007, **111**, 2951.
23 J. N. Clifford, G. Yahioglu, L. R. Milgrom and J. R. Durrant, *Chem. Commun.*, 2002, 1260.
24 A. J. Mozer, P. Wagner, D. L. Officer, G. G. Wallace, W. M. Campbell, M. Miyashita, K. Sunahara and S. Mori, *Chem. Commun.*, 2008, 4741.

